Structure and Dynamics in Polymer Blends: A ^{13}C CPMAS NMR Study of Poly(3-octylthiophene)/Poly(phenylene oxide)

Staffan Schantz* and Nils Ljungqvist

Department of Polymer Technology, Chalmers University of Technology, S-412 96 Göteborg, Sweden

*Received April 19, 1993; Revised Manuscript Received August 16, 1993**

ABSTRACT: We report ^{13}C CPMAS (cross-polarization magic angle spinning) NMR results from melt-mixed blends of undoped poly(3-octylthiophene) (POT) and poly(phenylene oxide) (PPO). The behavior of proton spin–lattice relaxation times in the rotating frame ($T_{1\rho}$(H)) and laboratory frame (T_1(H)) indicate that the blends are immiscible. Alkyl side-chain ^{13}C spin–lattice relaxation times (T_1(C)) increase considerably in blends of POT concentrations lower than ~30%, reflecting an increased molecular flexibility for POT. Changes in mobility are indicated also from dynamic mechanical measurements in which the maximum of the loss tangent for POT is found to shift to lower temperatures in the blends by ~5-15 K. We suggest that the increased mobility is caused by thermal stresses in the material.

Introduction

In 1977 doped polyacetylene was discovered to be highly conductive, and since then the research of so called "synthetic metals" has been very active.[1] Doped polypyrrole, polythiophene, and polyaniline are other examples of electron-conducting polymers. The large interest in these materials is mainly due to the possible combination of metallic conductivity and the good processability normally associated with polymeric materials. A wide variety of applications has been proposed, e.g., rechargeable batteries, EMI-shielding devices, and light-emitting diodes.[2] A problem, however, with some of these polymers is that their processing is difficult. This is because the stiffness of the conjugated chains make the materials insoluble and difficult to melt. Once concept, among others, to lower the melting transition and increase the solubility is to attach flexible side chains to the rigid backbone. Poly(3-alkylthiophene) (P3AT) is an example where alkyl side chains longer than butyl give rise to processability both in melt and in solution.[3–6] Similar behavior has also been reported for poly(3-alkylpyrroles) and poly(alkylphenylenes).[7,8] Apart from the technical applications for P3ATs, the conductivity mechanism as well as the complex structure and dynamics in these systems poses many challenging questions regarding the fundamental physics and chemistry.[9]

Since P3ATs are soluble and meltable it is possible to prepare blends with common bulk polymers. Recently, such blends have been investigated, e.g. poly(3-octylthiophene) (POT) mixed with poly(phenylene oxide) (PPO),[10,11] ethylene vinylacetate (EVA),[12,13] ethylene butylacrylate (EBA),[10,12] polycarbonate (PC),[10] polystyrene (PS),[9] and polyethylene (PE).[10,12] Some of the blends have relatively high conductivity (typically 10^{-4}–1 S cm^{-1}) for amounts of only ~10–30% of conducting material, see Figure 1. However, very little is known about the microscopic properties of blends with POT. Signs of interactions between the component polymers in POT/EVA blends have been reported.[13] For POT/PS small amounts of POT seem to dissolve in the matrix polymer as indicated by shifts in the glass transition temperature, T_g.[9] So far, however, in those POT blends investigated with thermal analysis, a single T_g has not been found, which indicates phase separation.

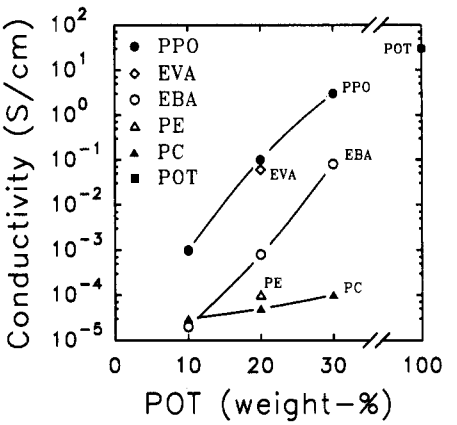

Figure 1. Conductivity vs concentration of POT for various blends doped with $FeCl_3$. Values for POT/PPO, POT/EBA, POT/PC, and POT/PE are from ref 10 and for POT/EVA from ref 12.

Among the various tools to study polymer blends, ^{13}C CPMAS NMR has proven very useful.[14–16] The technique is suitable for investigations of interactions on the molecular level, due to its high resolution in the solid state combined with the short-range nature of NMR. In addition, CPMAS relaxation times can provide information on sizes of microheterogeneities in blends. Through the process of spin diffusion, proton spin–lattice relaxation times in the laboratory frame (T_1(H)) and in the rotating frame ($T_{1\rho}$(H)) are strongly dependent on the domain sizes of the various components (in ^{13}C CPMAS NMR, the proton relaxation times can be detected indirectly from the ^{13}C signals).[17,18] The observation of a single proton T_1(H), between the T_1's of the component polymers, indicates phase sizes smaller than ~10 nm in the blend. If the polymers share a common $T_{1\rho}$(H), the blend is miscible or the separated phases, if present, are smaller than ~1 nm. For carbons, on the other hand, spin diffusion is limited due to the low natural abundance of ^{13}C nuclei.[15] Therefore, carbon spin–lattice relaxation times typically probe site-specific mobilities, and they are suitable for studies of the dynamics in polymer blends. Other approaches for investigating blends exist using solid-state NMR, e.g. two-dimensional techniques directly probing spin diffusion and various labeling methods.[16,19,20]

In the present study blends of undoped POT with PPO have been investigated using CPMAS NMR, electron microscopy techniques, and DMTA (dynamic mechanical

* Abstract published in *Advance ACS Abstracts*, October 15, 1993.

0024-9297/93/2226-6517$04.00/0 © 1993 American Chemical Society

thermal analysis). Proton and carbon relaxation time constants, as obtained by the CPMAS technique, have been used to study phase size and mobility. The POT/PPO system has been chosen since promising conductivity data has been reported for the corresponding doped blends: ~3 S cm^{-1} for a 30/70 (by weight)[10] POT/PPO blend at room temperature, see Figure 1, and preliminary NMR results indicate some degree of compatibility.[11]

Experimental Section

Materials. The POT used (provided by Neste Oy, Finland) was chemically synthesized with $FeCl_3$, according to the method developed by Sugimoto et al.[21] The weight- and number-average molecular weights of the polymer are M_w = 147 000 and M_n = 19 000. The residue of iron is less than 0.016% by weight, and no effects of paramagnetic ions on the NMR spectra or relaxation times were found in the blends. The poly(2,6-dimethyl-1,4-phenylene oxide) (PPO) was used as received (from Scientific Polymer Products). The M_w for PPO is 50 000. For appropriate comparisons, the homopolymers were subject to the same treatment as the blends, see below.

Blends of POT concentrations 10, 20, and 30 wt % were prepared by melt mixing in a Brabender Plasticorder (PLE 651). Due to the high melting point of PPO, the mixing temperature was 553 K and the mixing time was 5 min. Only a slight degradation was found after the heating procedure, as examined by the carbonyl infrared absorption band and by determination of the gel content (nonsoluble part in chloroform). No carbonyl resonances in the CPMAS spectra could be observed, which also can be taken as an indication of minor degradation.[22] Moreover, the various relaxation parameters of the homopolymers did not change, within the experimental accuracy, after the heat treatment. After blending, the samples were cooled to room temperature and thereafter dried (at 298 K) at low pressure for 24 h. A few blends were prepared also by a second method: precipitation from chloroform solutions using methanol as a nonsolvent. The precipitates were then filtered off, and the resulting powders were dried as above.

Electron Microscopy. SEM micrographs were obtained with a JEOL JSM-5300 scanning electron microscopy (employing 3000 times magnification in Figure 2). The distribution of POT phases in the blends was probed by X-ray mapping of sulfur atoms with EPMA/EDS technique (Electron Probe Micro Analyzer/Energy Dispersive Spectrometer) using a JEOL JXA-8600 electron probe combined with a Tracer Northern series II spectrometer. The resulting mapping images and the SEM micrographs were, respectively, taken from the same surface area of each sample. Samples were fractured at liquid nitrogen temperature. The fracture surfaces were then coated with thin carbon layers using carbon evaporation.

Thermal Analysis. DMTA tests were run on a Rheometrics RDA II at 1 Hz over the temperature range 223–533 K. The samples investigated were pressed at 573 K into ~1 mm thick films.

CPMAS NMR. Solid-state ^{13}C CPMAS NMR spectra were recorded at 75.4 MHz using a Varian VXR300 spectrometer equipped with a high-power amplifier and a Doty CPMAS probe. Samples were packed as powders in sapphire rotors with Kel-f endcaps and spun at 5 kHz. In the variable-temperature measurements, a Varian VT CPMAS probe was used (with silicon nitride rotors and torlon endcaps). Cross polarization was performed at 28 kHz (9-μs 90° pulses for both ^{13}C and ^{1}H), the proton decoupling strength was approximately 65 kHz, and the delay between successive acquisitions was 3–6 s. A fixed cross-polarization contact time of 0.5 or 3 ms was used in most of the experiments (except for in the $T_{1\rho}(H)$ measurements where the contact time was varied between 2 and 14 ms). Prior to Fourier transformation, the free induction decays were zero filled to 8k. The spectral width was 31 kHz, and the applied line broadening was 10 Hz. The magic angle was adjusted using KBr.[23] Chemical shifts were calibrated via external reference to the aromatic carbon of hexamethylbenzene (132.2 ppm relative to TMS). Following Haw and co-workers,[24,25] the sample temperature was calibrated using samarium acetate tetrahydrate and 1,4-diazabicyclo[2.2.2]-octane (DABCO).

Proton T_1's were measured using an inversion–recovery sequence (180°–τ–90°) followed by the ordinary cross-polarization scheme.[26] Rotating-frame relaxation times ($T_{1\rho}(H)$) were measured as the final slope of carbon intensity vs cross-polarization contact time.[14] Torchia's method[27] and a direct inversion–recovery sequence were used for measurements of carbon $T_1(C)$. In the latter pulse sequence, no cross polarization was employed and the delay between sequences was chosen to be longer than $5T_1$ (T_1 being the time constant for the slowest relaxing carbon nucleus). For each spectrum in the arrayed experiments, 1000–5000 transients were accumulated, repeatedly cycling through the different time values. The curve fittings of the various signal decays/recoveries were performed with Varian standard software (VnmrS 4.1B) and/or other standard nonlinear least-squares methods.

By considering the uncertainty in the sample temperature, statistical errors in curve fittings of semilog plots and the reproducibility, the experimental error in the various relaxation time constants is estimated to be less than ±10% (or otherwise explicitly given).

Results and Discussion

Electron Microscopy. SEM micrographs of the POT/PPO blends are presented in Figure 2a. The blends show a complex phase structure which changes significantly with composition. It is not straightforward to identify each polymer in the SEM micrographs. However, in Figure 2b X-ray mapping of sulfur atoms by EPMA/EDS analysis more clearly reveals the dispersion of POT in the PPO matrix (SEM and mapping images in Figure 2 correspond, respectively, to the same surface area of each sample). Sulfur-rich (i.e., POT-rich) regions are represented as bright dots in Figure 2b. The blend of lowest POT concentration (10/90) is homogeneous on the ca. μm-length scale of Figure 2. For the 20/80 blend a similar homogeneous phase structure can be seen, however, in coexistence with regions of higher POT content. Increasing the POT concentration further results in the formation of even larger POT-rich domains with sizes of the order ~1 μm (Figure 2b).

Thermal Analysis. In Figure 3 are shown results from DMTA measurements of POT, PPO, and their blends with focus on the glass transition region of POT. For temperatures above ~370 K, no changes were observed (this temperature region is not included in Figure 3) in the thermal data; the glass transition of PPO at 483 K is unaffected upon blending. The maximum of the loss tangent (tan δ) for POT appears around ~270 K in the blends, which is close to the value for the homopolymer, see Figure 3. This observation of two separate T_g's in the blends is a strong indication of phase separation for POT/PPO. A small shift, however, in the loss peak of POT is observed; the peak maximum shifts toward *lower* temperatures in the blends as compared to pure POT, see Figure 3. The shift increases for decreasing POT content below ~30% and for the 10/90 blend a shift of ~15 K is found. The results are somewhat surprising since any sign of compatibility, for example small amounts of POT dissolving into the PPO matrix, would be expected to shift T_g in the opposite direction. However, similar behavior has been reported for other systems, such as ABS resins,[28] POT/poly(3-dodecylthiophene),[29] and poly(ethylene oxide)/poly(*N*-vinylpyrrolidone) blends[30] (as seen in Figure 1 in ref 30, however, not discussed by the authors), i.e. a low-temperature shift in T_g for the mobile polymer component. Booij has discussed the effect in the case of ABS resins.[28] The large difference in thermal contraction in this system between the rubber phase and the plastic phase as the sample is cooled from the melt will set up stresses in the material, provided the phases are bonded

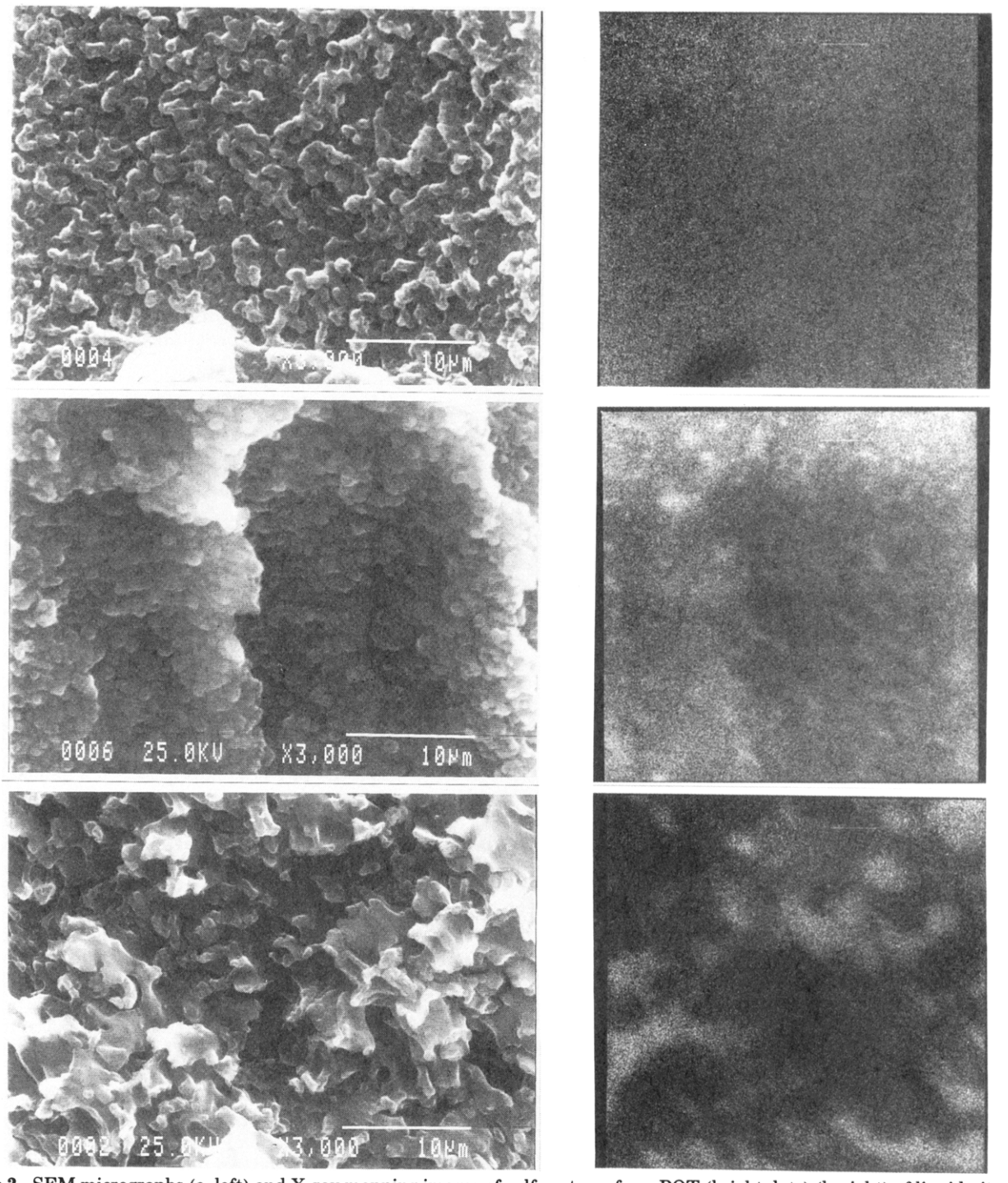

Figure 2. SEM micrographs (a, left) and X-ray mapping images of sulfur atoms from POT (bright dots) (b, right) of liquid nitrogen fractured surfaces of POT/PPO blends. The compositions are 10/90 (top), 20/80 (middle), and 30/70 (bottom). The SEM and mapping images are, respectively, taken from the same surface area for each sample.

together with sufficient strength (for example by grafting). This is because the rubber cannot contract to the same degree as it would without interaction with the matrix. The thermal stresses, in turn, will cause dilation of the rubber, i.e. increased flexibility, observed as a shift in T_g to lower temperatures. The magnitude of these thermal stresses increases as the temperature decreases and as the rubber content is lower. The difference between the T_g's of the two polymers should be at least 100–200 K (compare ~210 K for POT and PPO) to cause a measurable glass transition shift, and typical shifts in the loss peak for the rubber phase in ABS are ~15–5 K for rubber concentrations of ~5–24 vol %, i.e. similar to POT/PPO of the present study. We suggest that thermal stresses may be responsible for the experimental observations also in POT/PPO. This is supported by the CPMAS NMR results (see below).

^{13}C CPMAS NMR Spectra. ^{13}C CPMAS spectra of POT (thiophene carbons at 136, 133, 131, and 126 ppm; methylene carbons, 33, 31, and 24 ppm; methyl carbon, 15 ppm), PPO (1,4-quaternary carbons, 146 and 155 ppm; 2,6-quaternary carbons, 133 ppm; protonated aromatic carbons, 117 and 112 ppm; methyl carbons, 16 ppm), and a 30/70 (POT/PPO) blend are shown in Figure 4. The assignments of the carbon peaks are from refs 31 and 32. No changes in line shapes or chemical shifts of spectra were found for the blends relative to the homopolymers. The main-chain carbon peaks of POT are unfortunately too weak for reliable intensity measurements in the blends, see Figure 4. Therefore, only alkyl side-chain signals were

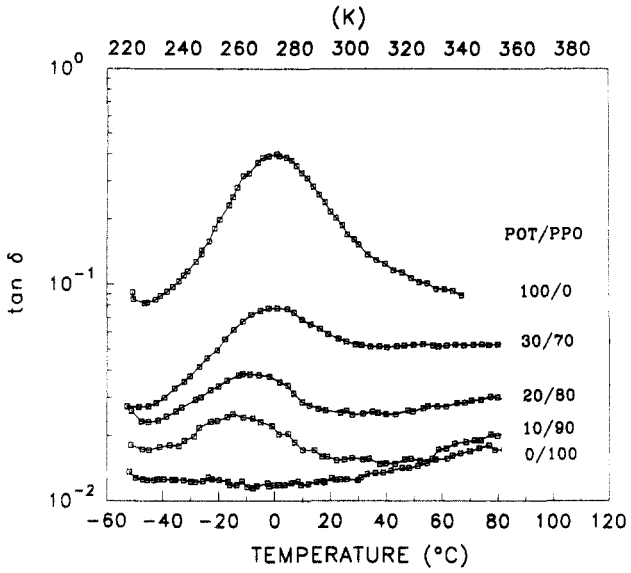

Figure 3. tan δ as a function of temperature for POT, PPO, and their blends of concentrations (POT/PPO) 100/0, 30/70, 20/80, 10/90, and 0/100.

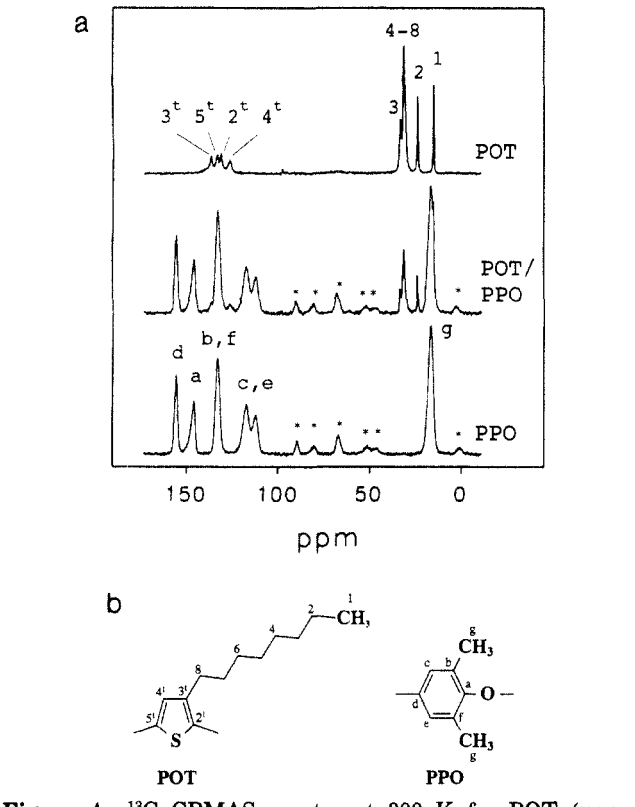

Figure 4. ^{13}C CPMAS spectra at 300 K for POT (upper spectrum), PPO (lower spectrum), and a 30/70 (POT/PPO) blend (middle spectrum) (a). Spinning side bands are marked with an asterisk (*). The assignments of the various carbon sites refer to the repeat unit structures shown in b.

used for relaxation time determinations of POT in the blends.

Relaxation Times in CPMAS NMR. The ^{13}C CPMAS technique can be employed to measure individual T_1's and $T_{1\rho}$'s for protons attached or close to various carbons. In principal, the proton relaxation times may then be used for studies of molecular motions since $T_{1\rho}(H)$ and $T_1(H)$ are sensitive to ca. kHz and ca. MHz mobilities, respectively. However, in solid polymers the proton relaxation is often perturbed by spin diffusion, i.e. propagation of magnetization by energy-conserving transitions of proton pairs having antiparallel spins (proton spin "flip-flops").[14-19] Because of this process, which tends to average different relaxations, all protons often share the same relaxation time and the individual relaxation characteristics are lost. In heterogeneous systems, however, the influence of spin diffusion on proton relaxation times can be very useful. For example, in a polymer blend all protons may average to a common relaxation time if the rate of spin diffusion (determined by the domain size and the spin diffusion constant) is large compared to the difference in relaxation rates between the component polymers. In this case the same relaxation time (single exponential) may be observed for all protons. Then, if the spin diffusion constant is known, relaxation data can be used to estimate domain sizes, using the fact that the maximum diffusion path length (L) is related to the diffusion constant (D) and the time over which the diffusion takes place (i.e. $T_{1\rho}(H)$ or $T_1(H)$) according to[17,18]

$$\langle L^2 \rangle \sim 6Dt \qquad (1)$$

For the present system D is not known, but we may use the approximation $D \sim \langle l_0^2 \rangle / T_2$, where l_0 is the distance between protons and T_2 is the proton spin–spin relaxation time.[17] Then, for the $T_1(H)$ data of the POT/PPO blends (see below), with $t = T_1(H) = 0.52$ s, $T_2 \sim 10$ μs and $l_0 \sim 0.1$ nm, eq 1 gives a value for the root-mean-square path length of ~56 nm. Similarly, we obtain ~8 nm for $T_{1\rho}(H) \sim 10$ ms (see below). Thus, for POT/PPO an averaged $T_1(H)$ or $T_{1\rho}(H)$ would indicate a domain size of less than 56 or 8 nm, respectively. Due to the relatively large uncertainty in the model used (for example, interfacial effects are neglected) and in T_2, these numbers should be taken as order of magnitude estimates.[18] Note also that the interpretations are valid only when the two homopolymers have different inherent relaxation times.

If instead the rate of spin diffusion is small compared to the difference in relaxation rates (large domains/small diffusion constant), the component polymers retain their relaxation behavior in the blend.[17,18] In this case the diffusion path length is less than the typical domain size. Partial averaging or multiexponential decays may result from situations intermediate between rapid and slow spin diffusion. It should be kept in mind that changes in mobility may also affect proton relaxation times with or without spin diffusion effects. The relative contributions of mobility and spin diffusion on relaxation are, however, difficult to obtain from proton relaxation measurements alone.

In contrast, carbon–carbon spin diffusion can in most cases be neglected due to the low natural abundance of carbon-13.[15] The carbon spin–lattice relaxation times are therefore sensitive probes of local mobilities. In systems with strongly coupled protons, $T_{1\rho}(C)$ (rotating-frame relaxation) may have nonmotional spin–spin (^1H–^{13}C) contributions, whereas $T_1(C)$ (laboratory frame) is not affected by spin–spin contributions.[33]

Proton $T_{1\rho}(H)$ Relaxation Times. The decay curves of ^{13}C signal intensity vs cross-polarization contact time are shown in Figure 5 for POT, POT20/PPO80, and PPO. The proton $T_{1\rho}(H)$'s are given by the respective inverse slope in Figure 5, see Table I. For the protons of POT the $T_{1\rho}$ values are similar and around 8 ± 2 ms. The methyl end group differs with a $T_{1\rho}(H)$ value of 13 ms, and the decay of the protonated thiophene carbon at 126 ppm (peak 4^t in Figure 4a) is biexponential in contrast to the other single-exponential decays. For amorphous PPO well below the glass transition, the proton $T_{1\rho}$'s are close to 18 ms (the 1-quaternary signal at 146 ppm, peak a in Figure 4a, gives a $T_{1\rho}(H)$ of 22 ms, thus deviating slightly from the other PPO values), indicating efficient spin diffusion in agreement with literature data (see Table I).[14,33]

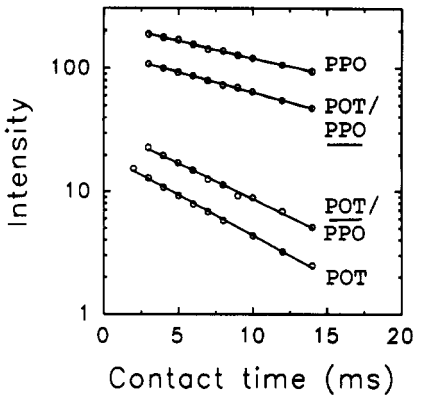

Figure 5. Signal intensity vs cross-polarization contact time at 300 K yielding proton $T_{1\rho}$'s for the methylene protons of POT (C4–C8 in Figure 4) and the aromatic protons of PPO (c, e in Figure 4). Results for the homopolymers and a 20/80 (POT/PPO) blend are shown. For clarity each line is begun at a separate origin on the y-axis.

Table I. Proton $T_{1\rho}$(H) Values for POT, PPO, and Their Blends at 300 K

	$T_{1\rho}$(H)[a] (ms)	
POT/PPO	POT[b]	PPO[c]
0/100		18
10/90	8.9 ● 1.2	17
20/80	9.9 ● 1.5	15
30/70	9.4	17
100/0	7.9	

[a] Estimated accuracy ±10% or otherwise explicitly given. [b] Average for the methylene protons of POT. [c] Average for all PPO protons.

In the blends the $T_{1\rho}$(H) values are essentially unchanged as compared to the homopolymers, see Figure 5 and Table I. Only slight changes of the relaxation times were found; the difference in $T_{1\rho}$(H) between POT and PPO decreases at most by a factor of ~2 upon blending. The relaxation behavior implies that the POT/PPO system is immiscible in the composition region investigated. This is in agreement with both the electron micrographs (Figure 2) and the DMTA results (Figure 3).

Proton T_1(H) Relaxation Times. Results of proton inversion–recovery cross-polarization measurements for POT, PPO, and their blends are presented in Figure 6. The calculated T_1(H) values are shown in Table II. The various recoveries are plotted as decays ($M_0 - M(t)$ vs delay time, where M_0 is the equilibrium magnetization) since in this presentation possible multiexponential behavior is more easily revealed than in the normal type of plot ($M(t)$ vs delay time). All decays were, however, found to be single-exponential, T_1(H) for POT and PPO is 0.22 and 0.42 s, respectively (Table II). Consequently, on the time scale of approximately 0.3 s, spin diffusion effectively averages all differences in T_1(H) for each homopolymer.

In contrast to the relatively small variations in $T_{1\rho}$(H), the proton T_1's change substantially in the blends as compared to the homopolymers, see Figure 6 and Table II. All protons relax with about the same time constant at room temperature, T_1(H) = 0.52 ± 0.02 s, in the blends of POT concentrations up to 20%. For the 30/70 blend the PPO relaxation time decreases to 0.40 s, i.e. close to the value for the homopolymer. The data seem to indicate spin diffusion between phases for blends of low POT contents. However, in the idealized picture of rapid spin diffusion, the averaged relaxation in a blend is weighted with the (proton) concentrations of the component polymers, i.e., the relaxation times for the blends should lie in between those of the pure polymers.[17,18] This is not the case for POT/PPO. The T_1(H) values in Figure 6 (Table

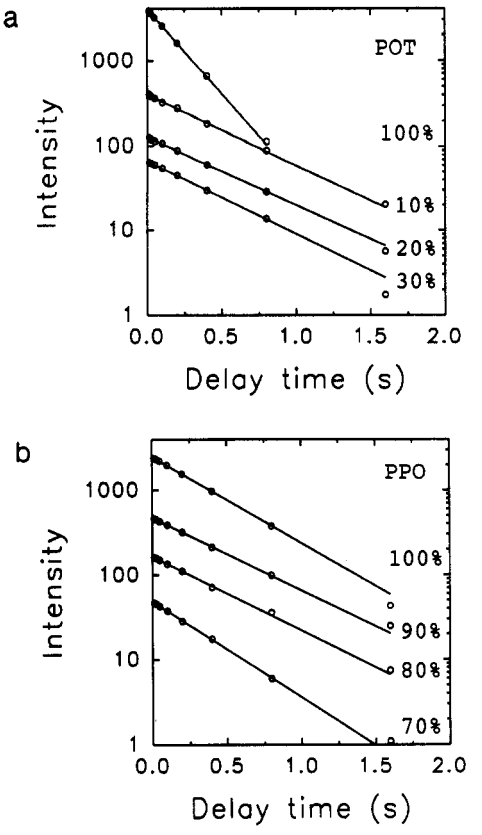

Figure 6. Results of proton inversion–recovery cross-polarization measurements at 300 K, plotted as $M_0 - M(t)$ vs delay time, yielding T_1(H)'s for the POT, PPO, and their blends of concentrations 10/90, 20/80, and 30/70 (POT/PPO). Results for POT are shown in (a) and for PPO in (b). For clarity each line is begun at a separate origin on the y-axis.

Table II. Proton T_1(H) Values for POT, PPO, and Their Blends at 300 K

	T_1(H)[a] (s)	
POT/PPO	POT[b]	PPO
0/100		0.42
10/90	0.52 ± 0.07	0.50
20/80	0.54 ± 0.08 (0.59 ± 0.09)[c]	0.50 (1.85 ± 0.28)[c]
30/70	0.50	0.40
100/0	0.22	

[a] Estimated accuracy ±10% or otherwise explicitly given. [b] For POT, the side-chain relaxation only could be measured in the blends. [c] Sample temperature 258 K.

II) are longer than those for both the homopolymers. As only one T_1(H) is observed (for POT concentrations lower than ~30%), this indicates that the intrinsic value of T_1-(H) for POT in the blend is longer than T_1(H) for pure POT. Thus, the dynamics of POT changes upon blending with PPO. Similar behavior of proton relaxation times has been reported for blends of poly(methylstyrene)/PPO[34] and PS/poly(vinyl methyl ether) (PVME).[35] Another complication for a simple interpretation of T_1(H) in terms of spin diffusion for POT/PPO is seen in Table II. Below room temperature the 20/80 blend does not share a common relaxation time, despite the fact that spin diffusion is more efficient at lower temperatures in general. At 258 K the T_1's are much different: 0.59 and 1.85 s for POT and PPO, respectively (see Table II).

The data in Table II may be explained as follows. For an averaging of relaxation times to occur, the rate of spin diffusion should be large compared to the difference in relaxation rates. Therefore, a small difference in relaxation rates (caused by a change in mobility of POT) at 300 K may be averaged by spin diffusion, whereas at lower

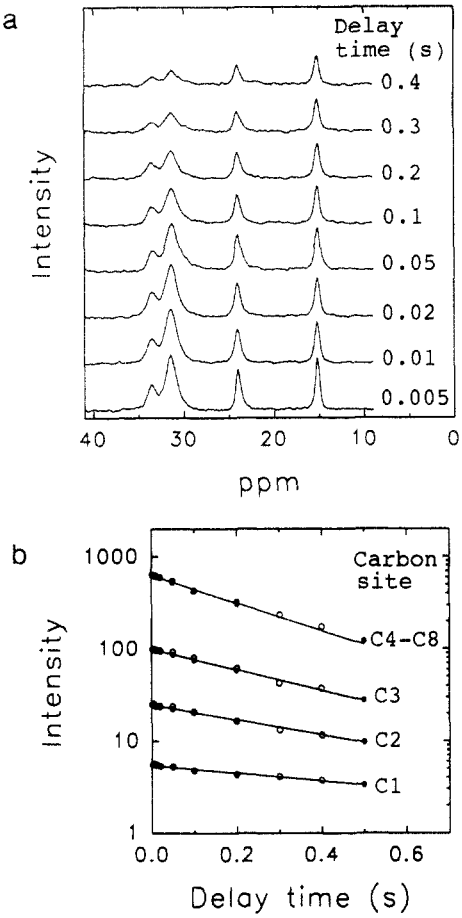

Figure 7. ^{13}C CPMAS spectra at 300 K for the alkyl side-chain carbons of POT at various delay times using the Torchia $T_1(C)$ carbon sequence (a). (b) Corresponding decay curves (see Figure 4 for carbon assignments) using the Torchia sequence (○) and an inversion–recovery sequence without cross polarization (●) (plotted as $M_0 - M(t)$ vs delay time). For clarity each line is begun at a separate origin on the y-axis.

temperatures the difference in relaxation rates is too large for efficient averaging. The assumption of rapid interdomain spin diffusion in deriving eq 1 does then not apply, indicating that mixing does not occur below a length scale of ~50–60 nm. This interpretation replaces an earlier one by the authors of $T_1(H)$ data at room temperature for POT/PPO blends.[11]

On the basis of the data in Table II, one might argue that a phase separation takes place when the temperature is decreased from 300 to 258 K. However, this explanation would require miscibility at room temperature, contradictory to the results from DMTA, $T_{1\rho}(H)$, and electron microscopy, which clearly show that the blends are not homogeneously mixed at 300 K. Moreover, the viscosity below room temperature is far too high for a phase separation to occur within practical time scales.

Carbon $T_1(C)$ Relaxation Times. To test the signs of changes in mobility for POT as obtained from other techniques, we have performed carbon $T_1(C)$ measurements which directly probe molecular mobility in the ~MHz region. Figure 7a shows a series of spectra from the side-chain region of POT as a function of the delay time using the Torchia $T_1(C)$ sequence.[27] The corresponding single-exponential decay curves are shown in Figure 7b, and the calculated $T_1(C)$ values are presented in Table III. At 300 K the relaxation is on the short correlation time side of the $T_1(C)$ minimum. This can be seen from the increasing $T_1(C)$ values for increasing distance (increased mobility) from the backbone, e.g., T_1-

Table III. Carbon $T_1(C)$ Values for the Alkyl Side Chain of POT at Various Temperatures (See Figure 4 for Peak Assignments)

	$T_1(C)^a$ (s)			
temp (K)	C4–C8	C3	C2	C1
300	0.30	0.36	0.46	1.05
341	0.34	0.61	0.63	1.29
361	0.42	0.87	1.05	1.35
381	0.71	1.03	2.61	3.15

[a] Estimated accuracy ±10%.

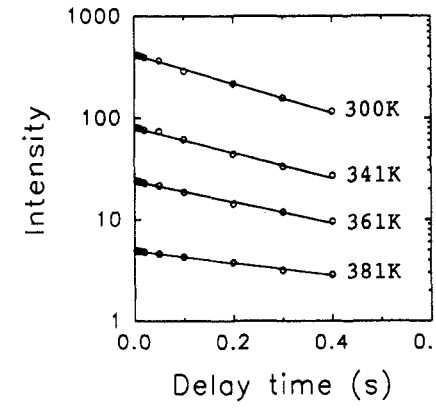

Figure 8. Experimental decay curves for the Torchia $T_1(C)$ sequence at various temperatures. The signal intensities are from the alkyl side-chain carbons of POT (C4–C8 in Figure 4). For clarity each line is begun at a separate origin on the y-axis.

(C) is 0.30 s for C4–C8 and 1.05 s for the methyl end group. Table III and Figure 8 include relaxation data at temperatures above room temperature, which confirm that the relaxation is on the fast side of the minimum. The high side-chain mobility (short correlation times that approach the motional narrowing limit), in fact, makes it possible to obtain direct ^{13}C high-resolution spectra using only MAS and broad-band decoupling with reasonably short pulse delays. Relaxation time measurements were therefore performed also with a second method: inversion–recovery sequence (180°–τ–90°) without cross polarization, see Figure 7b (plotted as $M_0 - M(t)$ vs delay time to give comparable decays). Note that the $T_1(C)$ data (as well as $T_{1\rho}(H)$) reflect the side-chain relaxation of POT, whereas the DMTA measurements (Figure 3) probe the main-chain relaxation observed at 284 K. Chen and Ni report a value of 206 K for the side-chain relaxation in POT from DMTA measurements at 1 Hz.[29] In the present DMTA investigations this low-temperature region was not investigated since the sub-T_g transition is too weak to be observed in the blends at low POT concentrations.

$T_1(C)$ data for POT, PPO, and their blends are shown in Figure 9 and Table IV. For PPO the decay for the nonprotonated aromatic carbons (peaks b, f in Figure 4) gives a $T_1(C)$ value of ~11 s which does not change in the blends (the T_1 values for PPO are qualitative due to the limited time range in Figure 9b, however, of importance is that no change could be observed for the blends). The same behavior was found for all the PPO carbons, i.e., an unchanged $T_1(C)$ relaxation. In contrast, the $T_1(C)$ values for the POT alkyl chains increase considerably in the blends. The 10/90 system shows the largest change, e.g., $T_1(C)$ for the C4–C8 methylene carbons increases from 0.30 ± 0.03 s in POT to 0.76 ± 0.15 s in the blend (Figure 9a and Table IV). Consequently, the mobility of side chains in POT increases in blends of low POT contents. For the other compositions, 20/80 and 30/70, the increase is smaller (see Table IV and Figure 9a) in agreement with the DMTA results.

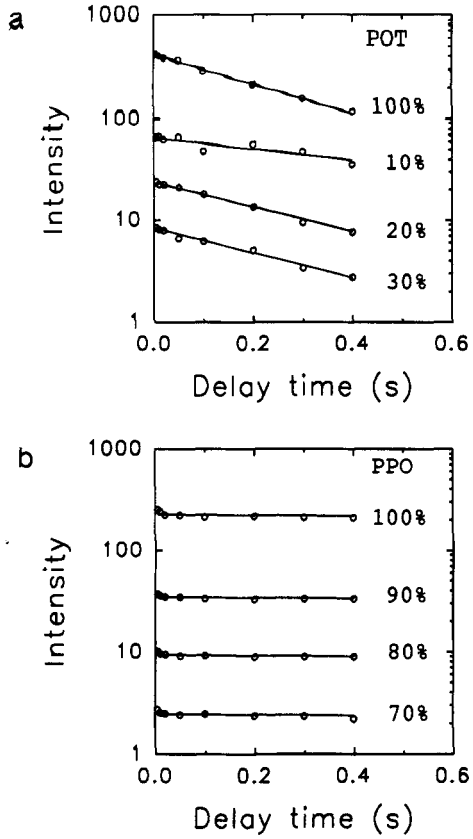

Figure 9. Experimental decay curves for the Torchia T_1(C) sequence at 300 K for POT, PPO, and their blends of concentrations 10/90, 20/80, and 30/70 (POT/PPO). Results for POT are shown in a and for PPO in b. For clarity each line is begun at a separate origin on the y-axis.

Table IV. Carbon T_1(C) Values for POT, PPO, and Their Blends at 300 K (See Figure 4 for Carbon Assignments)

	T_1(C)[a] (s)				
	POT[b]				
POT/PPO	C4–C8	C3	C2	C1	PPO[c] b, f
0/100					11
10/90	0.76 ± 0.15		0.74 ± 0.15		11
20/80	0.36	0.53	0.69		11
30/70	0.36	0.41	0.61		11
100/0	0.30	0.36	0.46	1.05	

[a] Estimated accuracy ±10% or otherwise explicitly given. [b] For POT, the side-chain relaxation only could be measured in the blends. [c] Qualitative values.

Next we discuss the observed mobility changes in terms of thermal stresses in the material. Such stresses may arise because of large differences in thermal contraction between the component polymers as a blend is cooled from the melt.[28] For the present blends the large difference in T_g (~200 K) enables POT to contract over a wide temperature range as the temperature is decreased from the molten state of the blend. The PPO matrix, on the other hand, cannot contract to the same degree because it passes the glass transition and solidifies at ~503 K. The subsequent dilation of the POT phases will increase the free volume and therefore the mobility. The effect increases for lower contents of POT, similar to observations in ABS resins and as predicted from an analysis of the thermal stresses for the latter system.[28] Moreover, a blend (10/90) prepared by precipitation from solution at room temperature shows completely different behavior from the corresponding melt-mixed blend. For the former sample no change of T_1(C) was found at 300 K; T_1(C) = 0.33 ± 0.03 s for the C4–C8 carbons in POT and 0.34 ± 0.07 s in the 10/90 blend (compare results for melt-mixed blends in Table IV). Since the NMR experiments were performed at about the same temperature as the sample preparation, no significant thermal contraction of the POT phases will be induced, and consequently, changes in mobility are not expected.

We note that for the melt-mixed blends a good contact between phases is required for dilation to occur. SEM micrographs (Figure 2a) show no sharp phase boundaries at low POT concentrations. In fact, it is not possible to identify the component polymer phases in the SEM images. Some weak interactions between POT and PPO may compatibilize the polymer phases into a nonequilibrium state by the high shear forces in the mixing procedure. Finally, we cannot rule out the possibility that a minor degradation has influenced the compatibility of the blends.

Conclusions

Proton $T_{1\rho}$(H) and T_1(H) data of melt-mixed POT/PPO blends suggest that mixing does not occur below a length scale of the order of ~50–60 nm, i.e., these blends are immiscible. With the exception of room temperature T_1-(H) relaxation, the component polymer relaxations are not averaged. At 300 K the T_1(H) values for POT in the blends differ from the T_1(H) value for the homopolymer. However, this difference appears to be mainly caused by a changed chain mobility. Interdomain spin diffusion seems to be a minor effect for the proton relaxations. DMTA results and electron micrographs support the interpretation of NMR data.

The alkyl side-chain dynamics for POT have been studied in detail with variable-temperature carbon T_1(C) measurements. At room temperature the T_1(C) relaxation is on the short correlation time side of the T_1(C) minimum, indicating a high flexibility. T_1(C) data for the blends show that the mobility of POT increases in melt-mixed blends (at low POT concentrations) but not in blends prepared from solution. In analogy with findings in rubber-modified amorphous plastics, the observed behavior may be explained by thermal stresses in the material. These stresses arise because of the large difference in thermal contraction between POT and PPO as the blend is cooled from the molten state. As a consequence, dilation of POT occurs and the mobility increases.

Acknowledgment. This work was carried out with the support of the Swedish Research Council for Engineering Sciences, the National Swedish Board for Technical Development and Neste Oy. The authors are grateful to Prof. Frans Maurer and Prof. Thomas Hjertberg for helpful discussions and to Hans Eklind who worked with the authors as part of his final-year undergraduate project. Finally, we would like to thank Annika Karlsson and Lars Eklund for their assistance in the DMTA and electron microscopy measurements, respectively.

References and Notes

(1) Chiang, C. K.; Finscher, C. R.; Park, Y. W.; Heeger, A. J.; Shirakawa, H.; Louis, E. J.; MacDiarmid, A. G. *Phys. Rev. Lett.* **1977**, *39*, 1098.
(2) *Handbook of Conducting Polymers*; Skotheim, T. A., Ed.; Marcel Dekker Inc.: New York, 1986; p 489.
(3) Jen, K. Y.; Oboodi, R.; Elsenbaumer, R. L. *Polym. Mater. Sci. Eng.* **1985**, *53*, 79.
(4) Yoshino, K.; Nakajima, S.; Fuji, M.; Sugimoto, R. *Polym. Commun.* **1987**, *28*, 309.
(5) Hotta, S.; Rughooputh, S. D. D. V.; Heeger, A. J.; Wudl, F. *Macromolecules* **1987**, *20*, 212.

(6) Kaner, R. B.; MacDiarmid, A. G. *Sci. Am.* **1988**, *258*, 60.
(7) Rühe, J.; Ezquerra, T. A.; Wegner, G. *Synth. Met.* **1989**, *28*, 177.
(8) Rehahn, M.; Schlüter, A.-D.; Wegner, G.; Feast, J. W. *Polymer* **1989**, *30*, 1054 and 1060.
(9) *Conjugated Polymers*; Bredas, J. L., Silbey, R., Eds.; Kluwer Academic Publishers: Dordrecht, 1991; p 315.
(10) Ljungqvist, N.; Hjertberg, T. *Synth. Met.* **1993**, *57*, 4944.
(11) Schantz, S.; Ljungqvist, N. *Synth. Met.* **1993**, *57*, 3483.
(12) Laakso, J.; Österholm, J.-E.; Nyholm, P.; Isotalo, H.; Stubb, H.; Inganäs, O.; Salaneck, W. R. *Synth. Met.* **1989**, *28* (1–2).
(13) Ho, K.-S.; Levon, K.; Mao, J.; Zeng, W.-Y.; Laakso, J. *Synth. Met.* **1993**, *57*, 3591.
(14) Stejskal, E. O.; Schaefer, J.; Sefcik, M. D.; McKay, R. A. *Macromolecules* **1981**, *14*, 275.
(15) Voelkel, R. *Angew. Chem., Int. Ed. Engl.* **1988**, *27*, 1468.
(16) Belfiore, L. A.; Lutz, T. J.; Cheng, C. In *Solid State NMR of Polymers*; Mathias, L. J., Ed.; Plenum Press: New York, 1991; Chapter 8, p 145.
(17) McBierty, V. J.; Douglass, D. C. *J. Polym. Sci.: Macromol. Rev.* **1981**, *16*, 295.
(18) Henrichs, P. M.; Tribone, J.; Massa, D. J.; Hewitt, J. M. *Macromolecules* **1988**, *21*, 1282.
(19) Blümich, B. *Adv. Mater.* **1991**, *3*, 237.
(20) Linder, M.; Henrichs, P. M.; Hewitt, J. M.; Massa, D. J. *J. Chem. Phys.* **1985**, *82*, 1585.
(21) Sugimoto, R.; Takeda, S.; Gu, H. B.; Yoshino, K. *Chem. Express* **1986**, *1*, 635.
(22) Abdou, M. S. A.; Xie, Z. W.; Leung, A. M.; Holdcroft, S. *Synth. Met.* **1992**, *52*, 159.
(23) Frye, J. S.; Maciel, G. E. *J. Magn. Reson.* **1982**, *48*, 125.
(24) Campbell, G. C.; Crosby, R. C.; Haw, J. F. *J. Magn. Reson.* **1986**, *69*, 191.
(25) Haw, J. F.; Crook, R. A.; Crosby, R. C. *J. Magn. Reson.* **1986**, *66*, 551.
(26) Sullivan, M. J.; Macial, G. E. *Anal. Chem.* **1982**, *54*, 1615.
(27) Torchia, D. A. *J. Magn. Reson.* **1978**, *30*, 613.
(28) Booij, H. C. *Br. Polym. J.* **1977**, *9*, 47.
(29) Chen, S.-A.; Ni, J.-M. *Makromol. Chem., Rapid Commun.* **1992**, *13*, 31.
(30) Cesteros, L. C.; Quintana, J. R.; Fernandez, J. A.; Katime, I. A. *J. Polym. Sci.* **1989**, *B27*, 2567.
(31) Stein, P. C.; Bolognesi, A. *Synth. Met.* Submitted for publication.
(32) Bielecki, A.; Burum, D. P.; Rice, D. M.; Karasz, F. E. *Macromolecules* **1991**, *24*, 4820.
(33) Schaefer, J.; Stejskal, E. O.; Buchdal, R. *Macromolecules* **1977**, *10*, 384.
(34) Dickinson, L. C.; Yang, H.; Chu, C.-W.; Stein, R. S.; Chien, J. C. W. *Macromolecules* **1987**, *20*, 1757.
(35) Chu, C. W.; Dickinson, L. C.; Chien, J. C. W. *J. Appl. Polym. Sci.* **1990**, *41*, 2311.